SOCIETY FOR EXPERIMENTAL BIOLOGY

Journal of Experimental Botany, Vol. 74, No. 17 pp. 5166–5180, 2023
https://doi.org/10.1093/jxb/erad195 Advance Access Publication 26 May 2023

RESEARCH PAPER

Soil nitrogen fertilization reduces relative leaf nitrogen allocation to photosynthesis

Elizabeth F. Waring[1,2], Evan A. Perkowski[1] and Nicholas G. Smith[1,*]

[1] Department of Biological Sciences, Texas Tech University, Lubbock, TX, USA
[2] Department of Natural Sciences, Northeastern State University, Tahlequah, OK, USA

* Correspondence: nick.smith@ttu.edu

Received 30 December 2022; Editorial decision 23 May 2023; Accepted 25 May 2023

Editor: Alistair Rogers, Brookhaven National Laboratory, USA

Abstract

The connection between soil nitrogen availability, leaf nitrogen, and photosynthetic capacity is not perfectly understood. Because these three components tend to be positively related over large spatial scales, some posit that soil nitrogen positively drives leaf nitrogen, which positively drives photosynthetic capacity. Alternatively, others posit that photosynthetic capacity is primarily driven by above-ground conditions. Here, we examined the physiological responses of a non-nitrogen-fixing plant (*Gossypium hirsutum*) and a nitrogen-fixing plant (*Glycine max*) in a fully factorial combination of light by soil nitrogen availability to help reconcile these competing hypotheses. Soil nitrogen stimulated leaf nitrogen in both species, but the relative proportion of leaf nitrogen used for photosynthetic processes was reduced under elevated soil nitrogen in all light availability treatments due to greater increases in leaf nitrogen content than chlorophyll and leaf biochemical process rates. Leaf nitrogen content and biochemical process rates in *G. hirsutum* were more responsive to changes in soil nitrogen than those in *G. max*, probably due to strong *G. max* investments in root nodulation under low soil nitrogen. Nonetheless, whole-plant growth was significantly enhanced by increased soil nitrogen in both species. Light availability consistently increased relative leaf nitrogen allocation to leaf photosynthesis and whole-plant growth, a pattern that was similar between species. These results suggest that the leaf nitrogen–photosynthesis relationship varies under different soil nitrogen levels and that these species preferentially allocated more nitrogen to plant growth and non-photosynthetic leaf processes, rather than photosynthesis, as soil nitrogen increased.

Keywords: Chlorophyll, J_{max}, leaf area, light availability, nutrient availability, photosynthetic capacity, V_{cmax}.

Introduction

Terrestrial photosynthesis is the largest flux of carbon between the atmosphere and the Earth's surface. As a result, the terrestrial biosphere component of Earth System Models (ESMs) is highly sensitive to representations of photosynthetic processes (Bonan *et al.*, 2011; Arneth *et al.*, 2012; Booth *et al.*, 2012; Smith and Dukes, 2013; Rogers *et al.*, 2017; Smith *et al.*,

Abbreviations, Chl_{area}, total leaf chlorophyll content per unit individual leaf area; J_{max}, the maximum rate of electron transport per unit individual leaf area; J_{max25}, the maximum rate of electron transport per unit individual leaf area standardized to 25 °C; M_{area}, leaf mass per unit individual leaf area; N_{area}, leaf nitrogen content per unit individual leaf area; N_{mass}, leaf nitrogen content per unit individual leaf mass; V_{cmax}, the maximum rate of Rubisco carboxylation per unit individual leaf area; V_{cmax25}, the maximum rate of Rubisco carboxylation per unit individual leaf area standardized to 25 °C; $\rho_{bioenergetics}$, the relative proportion of leaf nitrogen in bioenergetics; $\rho_{lightharvesting}$, the relative proportion of leaf nitrogen in light harvesting; $\rho_{rubisco}$, the relative proportion of leaf nitrogen in Rubisco.

2016, 2017; Ziehn *et al.*, 2011). The differential representation of these processes in ESMs (Rogers *et al.*, 2017) probably contributes the wide range of their projections of future terrestrial carbon uptake and storage (Keenan *et al.*, 2012; Friedlingstein *et al.*, 2014; Bonan *et al.*, 2019; Davies-Barnard *et al.*, 2020). The inability to consistently model these processes is in part due to incomplete understanding of the mechanisms driving photosynthetic responses to global change conditions (Knorr and Heimann, 2001; Smith and Dukes, 2013; Dietze, 2014; Rogers *et al.*, 2017).

Photosynthetic capacity in ESMs is often determined by the nitrogen content in leaves (Smith and Dukes, 2013; Rogers, 2014; Rogers *et al.*, 2017), following from the idea that much of the nitrogen in leaves is found in photosynthetic proteins (Evans, 1989; Evans and Seemann, 1989; Evans and Clarke, 2019) and the commonly observed positive relationship between leaf nitrogen and photosynthetic capacity (Field and Mooney, 1986; Wright *et al.*, 2005; Kattge *et al.*, 2009; Walker *et al.*, 2014). However, more contemporary analyses on a wider range of species suggests that the fraction of leaf nitrogen allocated to photosynthetic processes may be lower and more variable than previously suggested due to variations in nitrogen allocation to structural and non-structural tissue (Ghimire *et al.*, 2017; Onoda *et al.*, 2017; Luo *et al.*, 2021), which calls the generality of these relationships into question.

Another issue that complicates the use of leaf nitrogen to predict photosynthetic processes is the relationship between soil nitrogen and leaf nitrogen. Recent analyses of nitrogen addition experiments have suggested that leaf nitrogen increases when nitrogen is added to soils (Firn *et al.*, 2019; Li *et al.*, 2020; Liang *et al.*, 2020) and that this coincides with an increase in photosynthetic processes (Li *et al.*, 2020; Liang *et al.*, 2020). However, these leaf-level responses are typically more muted than responses seen at the whole-plant scale (e.g. increases in leaf area and above-ground biomass; LeBauer and Treseder, 2008; Fay *et al.*, 2015; Li *et al.*, 2020; Liang *et al.* 2020). The comparison of these results indicates that plant allocation responses may ultimately determine the link between soil and leaf nitrogen, as plants can use added soil nitrogen to boost leaf quality or quantity. This may also depend on other factors such as canopy light availability (Hikosaka, 2014) or species-specific costs to acquire nitrogen (Terrer *et al.*, 2018; Perkowski *et al.*, 2021).

Some studies have indicated that soil nitrogen availability is relatively unimportant for determining leaf nitrogen (Maire *et al.*, 2015; Dong *et al.*, 2017, 2020) and photosynthetic capacity (Ali *et al.*, 2015; Smith *et al.*, 2019; Peng *et al.*, 2021; Dong *et al.*, 2022), and that these traits are better predicted from above-ground climate alone. It is well known that above-ground variables such as light (Boardman, 1977; Poorter *et al.*, 2019), temperature (Berry and Bjorkman, 1980; Sage and Kubien, 2007; Yamori *et al.*, 2014), and CO_2 (Bazzaz, 1990; Poorter *et al.*, 2022) are dominant controls on photosynthetic capacity. However, plants need nitrogen from soils to build and maintain photosynthetic enzymes, which generally have high nitrogen requirements (Evans and Clarke, 2019). As a result, both soil-centric and climate-centric frameworks need to be unified to better understand linkages between soil nitrogen availability, leaf nitrogen, and photosynthetic capacity.

A possible unification theory for how soil nitrogen impacts leaf photosynthetic capacity under varying climates was proposed by Paillassa *et al.* (2020). The theory is based on optimization (Franklin *et al.*, 2020; Harrison *et al.*, 2021) and follows from earlier theoretical developments (Wright *et al.*, 2003; Prentice *et al.*, 2014; Maire *et al.*, 2015; Smith *et al.*, 2019). The theoretical framework suggests that climate determines leaf demand to build and maintain enzymes that drive leaf photosynthesis. Nitrogen is acquired and then allocated to photosynthetic leaf tissue to meet that demand. In such cases where leaf nitrogen demand is met, plants are then expected to allocate excess available nitrogen to build new plant tissues (e.g. leaves in an open canopy scenario) or increase leaf nitrogen as a means to increase water use efficiency (Paillassa *et al.*, 2020). While compelling, few direct tests of this theory exist outside of environmental gradient studies on a limited set of traits in leaves (Dong *et al.*, 2017, 2020; Paillassa *et al.*, 2020; Westerband *et al.*, 2023) and manipulation of soil symbionts (Bialic-Murphy *et al.*, 2021). No studies, to date, have tested the theory on whole-plant or within-leaf allocation processes under direct soil nitrogen manipulation.

Here, we measured leaf and whole-plant responses to nitrogen demand, created using a light availability gradient, and nitrogen availability, created using a soil nitrogen fertilization gradient, in a fully factorial greenhouse experiment. Responses were measured in a species without the ability to form associations with symbiotic nitrogen-fixing bacteria, cotton (*Gossypium hirsutum* L.), and a species with the ability to form associations with symbiotic nitrogen-fixing bacteria, soybean [*Glycine max* (L.) Merr]. This experiment was done in concert with the experiment described by Perkowski *et al.* (2021), using the same plants for both experiments. Perkowski *et al.* (2021) found that structural carbon costs to acquire nitrogen—the ratio of below-ground carbon allocation to whole-plant nitrogen uptake—increased with nitrogen addition due to a stronger increase in whole-plant nitrogen uptake than below-ground carbon allocation and decreased with increasing light availability due to a stronger increase in below-ground carbon allocation than whole-plant nitrogen uptake. Similar directional responses to nitrogen addition and light availability were observed in both species, though carbon costs to acquire nitrogen in *G. max* were anecdotally less sensitive to increasing fertilization than in *G. hirsutum*. Perkowski *et al.* (2021) speculated that this pattern may have been due to a reduction in root nodulation that prompted a switch away from nitrogen acquisition through nitrogen fixation and toward direct uptake with increasing fertilization.

In this study, we measured photosynthetic traits at the individual leaf level using gas exchange and quantified nitrogen allocation to different photosynthetic processes. At the whole-plant level, we measured leaf tissue production and whole-plant biomass. We quantified trade-offs between leaf and whole-plant physiological processes in response to fertilization and light availability treatments, contextualizing our results using patterns observed in Perkowski *et al.* (2021). Specifically, we tested the following hypotheses.:

(i) Increasing nitrogen demand (i.e. greater light availability) would increase leaf-level photosynthetic nitrogen, resulting in increased leaf-level photosynthetic capacity in both species and under all levels of nitrogen availability. We expected that increased light availability would result in increased whole-plant growth due, in part, to higher leaf-level photosynthesis, and would be further increased by greater leaf area and, thus, greater whole-plant photosynthesis.

(ii) Increasing soil nitrogen availability would not impact leaf-level photosynthetic processes because leaf demand for nitrogen would be met for all leaves. Instead, increasing soil nitrogen availability would increase total leaf tissue production as a means of maximizing whole-plant photosynthesis, resulting in greater biomass, due to reduced carbon costs to acquire nitrogen with increasing fertilization (Perkowski *et al.*, 2021).

(iii) *Gossypium hirsutum* would show a stronger total leaf area response to nitrogen availability than *G. max* because its whole-plant processes are more nitrogen limited due to its relatively high costs of nitrogen acquisition under low soil nitrogen availability (Perkowski *et al.*, 2021). However, we expected that the species differences would only be seen at the whole-plant level and not at the leaf level, as the ability to associate with symbiotic nitrogen-fixing bacteria should not directly modify leaf nitrogen demand.

Materials and methods

Greenhouse experimental design

Gossypium hirsutum and *Glycine max* were planted in individual 3 liter pots (NS-300; Nursery Supplies, Orange, CA, USA) containing a 3:1 mix of unfertilized potting mix (Sungro Sunshine Mix #2, Agawam, MA, USA) to native soil extracted from an agricultural field most recently planted with *G. max* at the USDA-ARS Laboratory in Lubbock, Texas (33.59°N, –101.90°W). The field soil was classified as Amarillo fine sandy loam (75% sand, 10% silt, 15% clay). Prior to planting, *G. max* seeds were inoculated with *Bradyrhizobium japonicum* (Verdesian N-Dure™ Soybean, Cary, NC, USA) to stimulate root nodulation. A total of 192 individuals per species were grown under similar, unshaded, ambient greenhouse conditions for 2 weeks to germinate and begin vegetative growth.

Three blocks were set up, each of which contained four light treatments created using shade cloth that reduced incoming radiation by either 0 (full sun), 30, 50, or 80%. Two weeks post-germination, individuals were randomly placed in one of the four light treatments in each block. Individuals received one of four nitrogen fertilization doses as 100 ml of a modified Hoagland solution (Hoagland and Arnon, 1950) equivalent to either 0 ppm N (0 mM N), 70 ppm N (5 mM N), 210 ppm N (15 mM N), or 630 ppm N (45 mM N) twice per week within each light treatment. Each Hoagland solution was modified to keep concentrations of other macro- and micronutrients equivalent (Table 1). Plants were routinely well watered to eliminate any water stress potential. Air temperature in the greenhouse house averaged 30.0 ± 3.2 °C with 50% relative humidity during the day, and 24.0 ± 1.2 °C with 30% relative humidity during the night. Within the light treatments, the mean ±SE daytime (10.00–16.00 h) photosynthetically active radiation (PAR) was 111 ± 4, 170 ± 5, 298 ± 10, and 397 ± 11 μmol m^{-2} s^{-1} for the 80, 50, 30, and 0% shade, respectively. The mean ±SE daily maximum PAR was 489 ± 10, 718 ± 12, 1124 ± 21, and 1662 ± 28 μmol m^{-2} s^{-1} for the 80, 50, 30, and 0% shade, respectively.

Gas exchange measurements

After 5 weeks of growth under the light and nitrogen treatments, we quantified the effects of light availability and nitrogen addition on whole-plant and leaf-level traits (n=12 for each light and nitrogen treatment combination).

Prior to harvesting individuals for biomass and leaf area, we attached a young, fully expanded, outer canopy leaf to a Li-COR 6800 portable photosynthesis machine (Li-COR Biosciences, Lincoln, NE, USA) and generated a carbon dioxide response curve under greenhouse saturated light conditions (1800 μmol m^{-2} s^{-1}) and constant chamber temperature (25 ℃) using the following reference carbon dioxide concentration (ppm) sequence: 400, 300, 200, 100, 50, 0, 400, 400, 600, 800, 1000, and 1200. Dark respiration was also measured after placing leaves in a dark chamber for 5 min to acclimate. We used these response curves and dark respiration rates to fit net photosynthesis (A_{net}) by intercellular CO_2 (C_i) curves (A_{net}/C_i curves) of each individual using the 'fitaci' function in the R package 'plantecophys' (Duursma, 2015), which estimates the maximum rate of Rubisco carboxylation (V_{cmax}; μmol m^{-2} s^{-1}) and the maximum rate of electron transport (J_{max}; μmol m^{-2} s^{-1}) based on the Farquhar *et al.* (1980) biochemical model of C_3 photosynthesis. The fitting was done using C_i, not mesophyll CO_2. The 'fitaci' function estimated the Michaelis–Menten coefficient for Rubisco as

Table 1. Summary table containing volumes of compounds used to create modified Hoagland solutions for each soil nitrogen fertilization treatment

Compound	0 ppm N	70 ppm N	210 ppm N	630 ppm N
1 M $NH_4H_2PO_4$	0	0.33	1	1
2 M KNO_3	0	0.67	2	2
2 M $Ca(NO_3)_2$	0	0.67	2	2
1 M NH_4NO_3	0	0.33	1	0
8 M NH_4NO_3	0	0	0	2
1 M KH_2PO_4	1	0.67	0	0
1 M KCl	4	1.33	0	0
1 M $CaCO_3$	4	3	0	0
2 M $MgSO_4$	1	1	1	1
10% Fe-EDTA	1	1	1	1
Trace elements	1	1	1	1

All volumes are expressed as milliliters of each solution per liter H_2O (ml l^{-1}).

$$K = K_c\left(1 + \frac{O_i}{K_o}\right) \quad (1)$$

where K_c (μmol mol^{-1}) and K_o (μmol mol^{-1}) are Michaelis–Menten coefficients of Rubisco activity for CO_2 and O_2, respectively, and O_i (210 000 μmol mol^{-1}) is the intercellular O_2 concentration. Leaf temperature-corrected values of K and the CO_2 compensation point (Γ^*) were calculated using the equations and parameters of Bernacchi *et al.* (2001).

Because leaf temperatures varied slightly from 25 °C (mean ±SD: 26.1 ± 1.5 °C), V_{cmax} and J_{max} were standardized to values at a leaf temperature of 25 °C (i.e. V_{cmax25} and J_{max25}, respectively) using equations from Kattge and Knorr (2007), assuming an acclimated temperature of 32 °C (average daytime temperature in the greenhouse throughout the experiment) as

$$f(T) = e^{\frac{H_a\left(T_{leaf}-298.15\right)}{RT_{leaf}298.15}}\frac{1 + e^{\frac{298.15(\Delta S)-H_d}{R298.15}}}{1 + e^{\frac{T_{leaf}(\Delta S)-H_d}{RT_{leaf}}}} \quad (2)$$

and

$$k_{25} = \frac{k_{Tleaf}}{f(T)} \quad (3)$$

where k is the rate of V_{cmax} or J_{max} at the leaf temperature (k_{Tleaf}) or at 25 °C (k_{25}), H_a is the activation energy (71 513 J mol^{-1} and 49 884 J mol^{-1} for V_{cmax} and J_{max}, respectively), R is the universal gas constant (8.314 J mol^{-1} K^{-1}), H_d is the deactivation energy (200 000 J mol^{-1}), and ΔS is the entropy term that characterizes the changes in reaction rate caused by substrate concentration (J mol^{-1} K^{-1}). ΔS was assumed to be a function of the acclimated temperature in Kelvin (T_{acc}; 305.15 K) as

$$\Delta S = a_{\Delta S}T_{acc} + b_{\Delta S} \quad (4)$$

where $a_{\Delta S}$ is the slope of the relationship (assumed to be 1.07 and 0.70 for V_{cmax} and J_{max}, respectively) and $b_{\Delta S}$ is the intercept of the relationship (assumed to be 668.39 and 659.70 for V_{cmax} and J_{max}, respectively) (Kattge and Knorr, 2007).

Leaf nitrogen allocation and chlorophyll content

The focal leaf used to generate each CO_2 response curve was harvested upon the completion of each curve. Three leaf discs were removed from each focal leaf for chlorophyll analysis. Scans of the focal leaf and leaf discs were curated using a flatbed scanner, and total areas of the focal leaf and leaf discs were analyzed using ImageJ (Schneider *et al.*, 2012). The focal leaf was placed in a drying oven set to 65 °C, then weighed after at least 48 h in the drying oven to obtain dry focal leaf biomass. The leaf mass per area (M_{area}; g m^{-2}) was determined by dividing dry leaf biomass by fresh focal leaf area.

Dry focal leaf biomass was then ground and homogenized for elemental combustion analysis. Leaf nitrogen content (N_{mass}; gN g^{-1}) was determined with subsamples of ground and homogenized focal leaf biomass using an elemental analyzer (Costech 4010; Costech, Inc., Valencia, CA, USA). Leaf nitrogen content was then converted to leaf nitrogen per unit leaf area (N_{area}; gN m^{-2}) by multiplying N_{mass} by M_{area}.

Leaf discs were placed in 10 ml of DMSO and incubated at 65 °C for 1 h (Barnes *et al.*, 1992). The chlorophyll content was measured using a spectrophotometer at 649.1 nm and 665.1 nm, and then calculated by using the equations described by Wellburn (1994):

$$Chl_a = 12.19A_{665} - 3.45A_{649} \quad (5)$$

and

$$Chl_b = 21.99A_{649} - 5.32A_{665} \quad (6)$$

where Chl_a is total Chl *a* content (μg ml^{-1}) and Chl_b is total Chl *b* content (μg ml^{-1}). Chl_a and Chl_b were converted to molar amounts by dividing each value by the molecular mass of chlorophyll (893.51 g mol^{-1} for Chl_a and 907.47 g mol^{-1} for Chl_b) and subsequently multiplying by the volume of the DMSO extractant (10 ml). Total chlorophyll content was calculated by adding molar amounts of Chl_a and Chl_b. Total chlorophyll content was converted to area- (Chl_{area}; mmol m^{-2}) and mass- (Chl_{mass}; mmol g^{-1}) based amounts using the weight and area of the discs.

Within-leaf nitrogen proportions

To examine the relative proportion of leaf nitrogen in Rubisco ($\rho_{rubisco}$; gN gN^{-1}), bioenergetics ($\rho_{bioenergetics}$; gN gN^{-1}), and light harvesting ($\rho_{lightharvesting}$; gN gN^{-1}), we first used a biochemical model (Niinemets and Tenhunen, 1997; Niinemets *et al.*, 1998) to calculate each proportion where

$$\rho_{rubisco} = \frac{V_{cmax25}N_r}{N_{area}V_{cr}} \quad (7)$$

where N_r is the amount of nitrogen in Rubisco, assumed to be 0.16 gN (g Rubisco)$^{-1}$, and V_{cr} is the specific activity of Rubisco, assumed to be 20.5 μmol CO_2 (g Rubisco)$^{-1}$ s^{-1} at 25 °C and

$$\rho_{bioenergetics} = \frac{J_{max25}N_b}{N_{area}J_{mc}} \quad (8)$$

where N_b is the amount of nitrogen in cytochrome *f*, assumed to be 0.1240695 g N (μmol cytochrome *f*)$^{-1}$, and J_{mc} is the capacity of electron transport per cytochrome *f*, set to 156 μmol electron (μmol cytochrome *f*)$^{-1}$ s^{-1} and

$$\rho_{lightharvesting} = \frac{Chl_{mass}}{N_{mass}C_b} \quad (9)$$

where C_b is the chlorophyll binding of the thylakoid protein complexes, assumed to be 2.75 mmol chlorophyll (g chlorophyll N)$^{-1}$. Note that because V_{cmax25} was estimated from C_i rather than mesophyll CO_2, the estimated V_{cmax25} and $\rho_{rubisco}$ are likely to be slight underestimates of the true values, but we do not expect this method of estimation to impact reported treatment responses.

Whole-plant measurements

Leaves, stems, roots, and root nodules were harvested upon completion of gas exchange measurements. Fresh leaf area was determined for all fully expanded leaves using a flatbed scanner to curate images and ImageJ to process leaf areas (Schneider *et al.*, 2012). We calculated total fresh leaf area as the sum of all leaf areas, including the area of the focal leaf used to curate gas exchange measurements. We then placed all organs into a

drying oven set to 65 °C for at least 48 h before weighing all organ material to determine dry biomass. Whole-plant biomass was calculated as the sum of leaf, stem, and root dry biomass for each individual. Root nodule biomass was not factored into the whole-plant biomass calculation. The biomass:pot volume ratio was <1 g l^{-1} (Poorter *et al.*, 2012) for all treatments except the 0% shading, 630 ppm N treatment in both species, where the average ratio was 1.24 g l^{-1} and 1.34 g l^{-1} for *G. max* and *G. hirsutum*, respectively (see Perkowski *et al.*, 2021).

Statistical analyses

We explored the effects of light availability, nitrogen availability, and plant species on leaf-level and whole-plant level processes using linear mixed-effects models. All models included plant species, shade cover, nitrogen fertilization, and their interactions as fixed effects, and block as a random intercept term. Species and block were used as categorical effects, while shade cover and nitrogen fertilization were used as continuous predictors. To examine treatment effects on leaf nitrogen, we fit models with dependent variables M_{area}, N_{mass}, and N_{area} with this structure. Each variable was natural log transformed before fitting to meet residual normality assumptions. Residual normality assumptions were assessed visually using residual versus fitted plots. To examine treatment effects on the photosynthetic process and components, we fit models with dependent variables V_{cmax25}, J_{max25}, and Chl_{area} with this structure. V_{cmax25} and J_{max25} were natural log transformed before fitting to meet normality assumptions. Next, to examine the treatment effects on the relative proportion of leaf nitrogen allocated to photosynthetic components, we fit models with dependent variables $\rho_{rubisco}$, $\rho_{bioenergetics}$, and $\rho_{lightharvesting}$ with this structure. Finally, to examine treatment effects on whole-plant metrics, we fit models with dependent variables of biomass (g) and total leaf area (m^2) with this model structure. Each variable was natural log transformed before fitting to meet normality assumptions.

We used the 'lmer' function in the 'lme4' R package (Bates *et al.*, 2015) to fit each model and used the 'Anova' function in the 'car' R package (Fox and Weisberg, 2019) to calculate Wald's χ^2 to determine the significance (α=0.05) using Type II ANOVA (Langsrud, 2003) of each fixed effect coefficient. Finally, we used the 'emmeans' R package (Lenth, 2016) to conduct post-hoc comparisons of categorical variables using Tukey's tests. Degrees of freedom for Tukey's test were approximated using the approach explained in Kenward and Roger (1997). All analyses and plots were done in R version 4.0.5 (R Core Team, 2019).

Results

Leaf mass per area and leaf nitrogen

A significant species by shading effect indicated that shading reduced M_{area}, but this reduction was greater in *G. hirsutum* than in *G. max* (P<0.01; Table 2; Fig. 1). The slope difference between species was confirmed by a post-hoc comparison of slopes (P<0.05). M_{area} was also greater in *G. hirsutum* than in *G. max* (P<0.001; Table 2; Fig. 1).

There was a three-way interaction between species, shading treatment, and fertilizer treatment for N_{mass} (P<0.01; Table 2; Fig. 1). Post-hoc tests indicated a positive effect of nitrogen fertilization on N_{mass} at all shade levels in *G. hirsutum* (P<0.05 in all cases; Fig. 1), but no fertilizer effect at any shade level for *G. max* (P>0.05 in all cases; Fig. 1). Post-hoc tests also indicated that shading had a positive effect on N_{mass} in both species under the lowest three nitrogen fertilization levels (P<0.05 in all cases). However, the shading effect was non-significant for *G. max* at the highest nitrogen fertilization level (P>0.05; Fig. 1) and significantly positive for *G. hirsutum* at the highest nitrogen fertilization level (P<0.05; Fig. 1).

A significant interaction between species and nitrogen fertilizer treatment indicated that the positive effect of nitrogen fertilizer on N_{area} was stronger for *G. hirsutum* than for *G. max* (P<0.001; Table 2; Fig. 1). However, post-hoc tests confirmed that the slope of the average N_{area} response to nitrogen fertilization was significantly positive for both species (P<0.05 in both cases; Fig. 1). We also used post-hoc tests to investigate a significant interaction between shading treatments and nitrogen fertilizer treatments (P<0.05; Table 2). These tests indicated that the significantly positive response of N_{area} to soil nitrogen fertilization was reduced with increasing shading; however, the response was significantly negative across all treatments (P<0.05; Fig. 1). This decreasing trend was probably driven by *G. max* (Fig. 1).

Leaf photosynthetic components

There was an interaction between species and nitrogen fertilizer treatment for V_{cmax25} (P<0.01; Table 3; Fig. 2), which post-hoc tests of slopes indicated was driven by a significantly positive effect of soil nitrogen fertilization for *G. hirsutum* (P<0.05; Fig. 2), but no effect in *G. max* (P>0.05; Fig. 2). V_{cmax25} also significantly decreased with increased shading (P<0.001; Table 3; Fig. 2) in both species and was significantly higher for *G. hirsutum* than for *G. max* on average across treatments (P<0.001; Table 3; Fig. 2).

There was an interaction between species and nitrogen fertilizer treatment for J_{max25} (P<0.01; Table 3; Fig. 2), which post-hoc tests of slopes indicated was driven by a significantly positive effect of soil nitrogen fertilization for *G. hirsutum* (P<0.05; Fig. 2), but no effect in *G. max* (P>0.05; Fig. 2).

Table 2. ANOVA results for linear mixed effects model fit for dependent variables M_{area} (g m^{-2}), N_{mass} (gN g^{-1}), and N_{area} (g m^{-2})

		M_{area}		N_{mass}		N_{area}	
	df	χ^2	*P*-value	χ^2	*P*-value	χ^2	*P*-value
Species (Sp)	1	970.976	**<0.001**	410.009	**<0.001**	80.153	**<0.001**
Shading (Sh)	1	605.128	**<0.001**	22.507	**<0.001**	248.874	**<0.001**
Fertilizer (F)	1	0.849	0.357	71.481	**<0.001**	56.544	**<0.001**
Sp×Sh	1	7.068	**0.008**	0.469	0.493	2.816	0.093
Sp×F	1	2.640	0.104	48.791	**<0.001**	19.193	**<0.001**
Sh× F	1	0.050	0.823	9.741	**0.002**	4.048	**0.044**
Sp×Sh×F	1	1.015	0.314	8.721	**0.003**	1.593	0.207

df=degrees of freedom, χ^2=Wald's chi-squared statistic. *P*-values <0.05 are in bold.

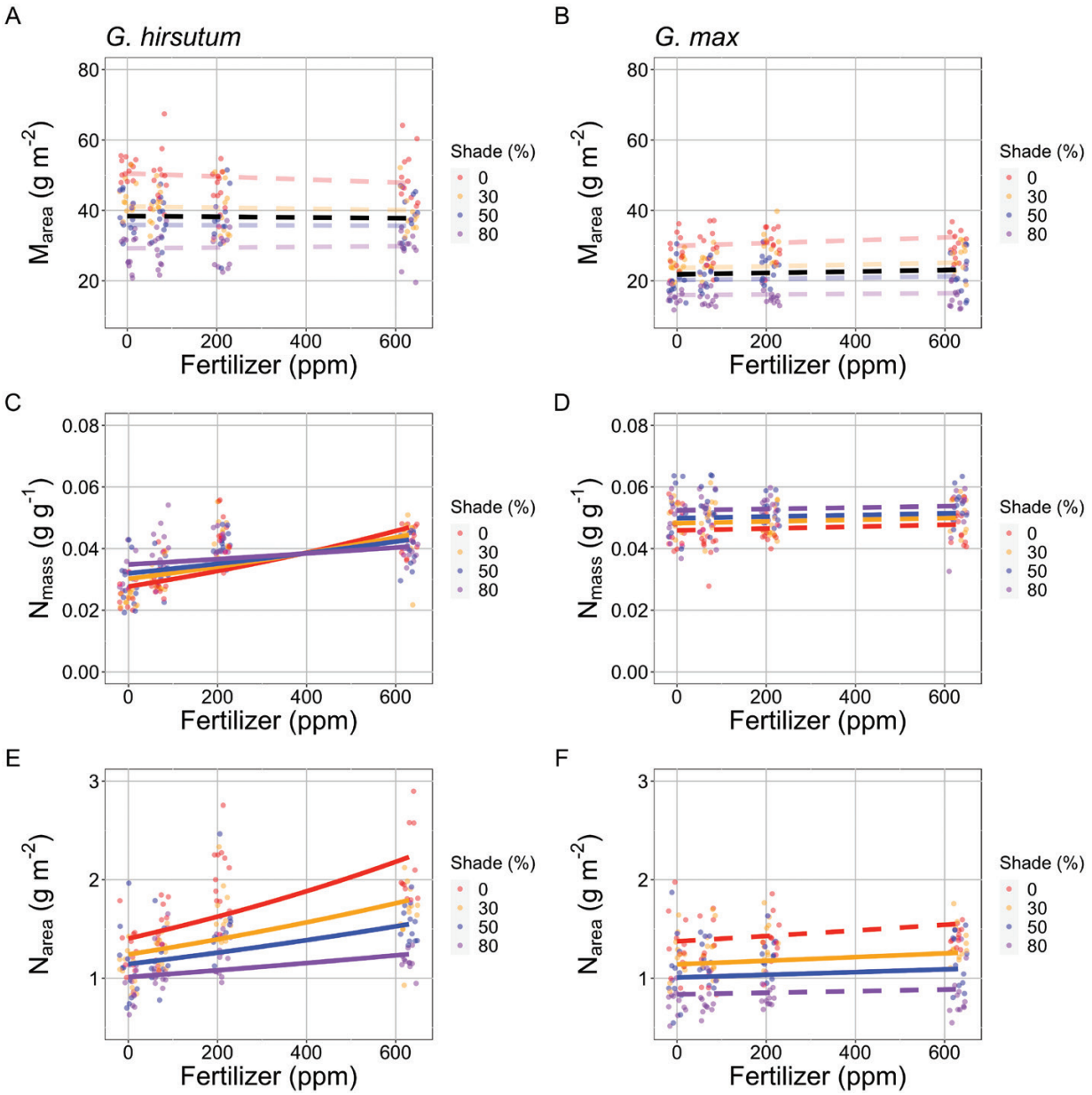

Fig. 1. The response of *G. hirsutum* (left panels) and *G. max* (right panels) M_{area} (A, B), N_{mass} (C, D), and N_{area} (E, F) to nitrogen fertilization in the 0% (red), 30% (orange), 50% (blue), and 80% (purple) shade treatments. The dots represent individual data points and the lines are fitted lines from the linear mixed effects models at each shade treatment value. Solid lines are statistically significant trends ($P<0.05$) and dashed lines are non-significant trends ($P>0.05$). Separate lines are plotted for each shading treatment, with colors corresponding to the shading treatments. In cases where no fertilizer treatment by shading treatment interaction effect existed (Table 2), a black line is plotted to show the average trend across shading treatments for each species, and per shading treatments are shown as transparent lines. Nitrogen fertilizer amount (*x*-axis) is in parts per million (ppm) added twice per week and is jittered for visibility.

There was also an interaction between species and shading treatment for J_{max25} ($P<0.05$). Post-hoc tests of slopes indicated that J_{max25} significantly decreased with shading in both species, but the decrease was stronger in *G. hirsutum* than in *G. max* ($P<0.05$; Fig. 2). J_{max25} was higher in *G. hirsutum* than in *G. max* on average across treatments ($P<0.05$; Table 3; Fig. 2).

There was an interaction between species and nitrogen fertilizer treatment for Chl_{area} ($P<0.01$; Table 3; Fig. 2), which post-hoc tests of slopes indicated was driven by a significantly positive effect of soil nitrogen fertilization for *G. hirsutum* ($P<0.05$; Fig. 2), but no effect in *G. max* ($P>0.05$; Fig. 2). There was also an interaction between species and shade treatment for Chl_{area} ($P<0.05$; Table 3; Fig. 2), which post-hoc tests of slopes indicated was driven by a significantly negative effect of shading for *G. max* ($P<0.05$; Fig. 2), but no effect for *G. hirsutum* ($P>0.05$; Fig. 2). Chl_{area} was

Table 3. ANOVA results for linear mixed effects model fit for dependent variables V_{cmax} (μmol m^{-2} s^{-1}), J_{max} (μmol m^{-2} s^{-1}), and Chl_{area} (mmol m^{-2})

		V_{cmax25}		J_{max25}		Chl_{area}	
	df	χ^2	*P*-value	χ^2	*P*-value	χ^2	*P*-value
Species (Sp)	1	22.208	**<0.001**	5.940	**0.015**	178.787	**<0.001**
Shading (Sh)	1	334.370	**<0.001**	592.324	**<0.001**	34.818	**<0.001**
Fertilizer (F)	1	12.712	**<0.001**	18.158	**<0.001**	11.413	**0.001**
Sp×Sh	1	1.037	0.308	4.974	**0.026**	8.582	**0.003**
Sp× F	1	10.620	**0.001**	7.366	**0.007**	31.115	**<0.001**
Sh×F	1	2.306	0.129	2.910	0.088	3.403	0.065
Sp×Sh×F	1	0.092	0.762	0.373	0.541	1.297	0.255

df=degrees of freedom, χ^2=Wald's chi-squared statistic. *P*-values <0.05 are in bold.

greater for *G. hirsutum* than for *G. max* ($P<0.001$; Table 3; Fig. 2).

Proportion of leaf nitrogen in photosynthetic components

The leaf nitrogen and photosynthetic treatment responses reported above resulted in a reduction in $\rho_{rubisco}$, $\rho_{bioenergetics}$, and $\rho_{lightharvesting}$ with increasing soil nitrogen fertilization ($P<0.01$ in all cases; Table 4; Fig. 3), with no interaction between fertilization treatment and species or shade treatment ($P>0.05$ in all cases; Table 4; Fig. 3). When totaled, this represents a reduction of 0.066 g of nitrogen used in photosynthesis per g of nitrogen in the leaf in the highest soil nitrogen treatment relative to the lowest soil nitrogen treatment, or an 11.5% reduction.

$\rho_{rubisco}$ and $\rho_{bioenergetics}$ were also both reduced by the shading treatments ($P<0.001$ in all cases; Table 4; Fig. 3). There was no effect of the shading treatments on $\rho_{lightharvesting}$ ($P>0.05$; Table 4; Fig. 3). $\rho_{lightharvesting}$ was greater for *G. hirsutum* than for *G. max* ($P<0.05$; Table 4; Fig. 3), while $\rho_{rubisco}$ and $\rho_{bioenergetics}$ were greater in *G. max* than in *G. hirsutum* ($P<0.05$; Table 4; Fig. 3).

Whole-plant leaf area and biomass

An interaction between shading and nitrogen fertilization treatments ($P<0.05$) indicated that, while soil nitrogen generally had a positive effect on total leaf area, this effect was reduced with increased shading (Table 5; Fig. 4). Post-hoc slope tests indicated that the soil nitrogen effect on total leaf area was positive in all species ($P<0.05$) and all shade combinations except for *G. hirsutum* under the highest shading level ($P>0.05$; Fig. 4). An interaction between shade treatment and species ($P<0.05$) indicated that shading reduced total leaf area in both species, but to a greater degree in *G. hirsutum* than in *G. max* (Fig. 4).

The biomass responses closely mimicked the total leaf area responses. Specifically, an interaction between shading and nitrogen fertilization treatments ($P<0.05$) indicated that, while soil nitrogen generally had a positive effect on total leaf area, this effect was reduced with increased shading (Table 5; Fig. 4). Post-hoc slope tests indicated that the soil nitrogen effect on total leaf area was positive in all species ($P<0.05$) and shade combinations except for *G. hirsutum* under the highest shading level ($P>0.05$; Fig. 4). An interaction between shade treatment and species ($P<0.01$) indicated that shading reduced total leaf area in both species, but to a greater degree in *G. hirsutum* than in *G. max* (Fig. 4).

Discussion

We used a manipulation experiment to test hypotheses regarding the connection between soil nitrogen, leaf nitrogen, and photosynthetic processes, as well as the connection and relationship to light availability. Counter to our second hypothesis, we found that soil nitrogen fertilization tended to increase leaf nitrogen (Fig. 1) and photosynthetic processes (Fig. 2), particularly in the non-nitrogen-fixing *G. hirsutum*. However, the relative proportion of leaf nitrogen in each of the photosynthetic processes examined (Rubisco, bioenergetics, and light harvesting) decreased with increasing nitrogen fertilization (Fig. 3). This pattern indicated that there was a change in the leaf nitrogen–photosynthesis relationship with increased soil nitrogen. Alternatively, photosynthetic processes were strongly and consistently stimulated by greater light availability (Fig. 2), in support of our first hypothesis and as shown by previous studies and theory (Boardman, 1977; Evans and Poorter, 2001; Niinemets *et al.*, 2015; Luo and Keenan, 2020). Whole-plant processes (total leaf area and biomass) were more consistently and positively stimulated by soil nitrogen availability regardless of species (Fig. 4), contrary to the species-specific responses expected in our third hypothesis. This suggests that the plants in this experiment were preferentially allocating additional nitrogen to the growth of new tissues over modifications of existing leaf tissue, supporting our second hypothesis. We expand and contextualize these results in the sections below.

Proportion of leaf nitrogen in photosynthesis decreases with soil nitrogen availability

We found that increasing soil nitrogen availability increased area-based leaf nitrogen (N_{area}) in both species (Fig. 1), corroborating previous results from fertilization studies (Firn *et al.*, 2019; Li *et al.*, 2020; Liang *et al.*, 2020). This happened alongside a slight stimulation of photosynthetic processes in the non-nitrogen-fixing *G. hirsutum* (Fig. 2). This result provides some support for the positive linkage between soil nitrogen, leaf nitrogen, and photosynthetic processes (Kattge *et al.*, 2009; Walker *et al.*, 2014). However, the lack of an effect

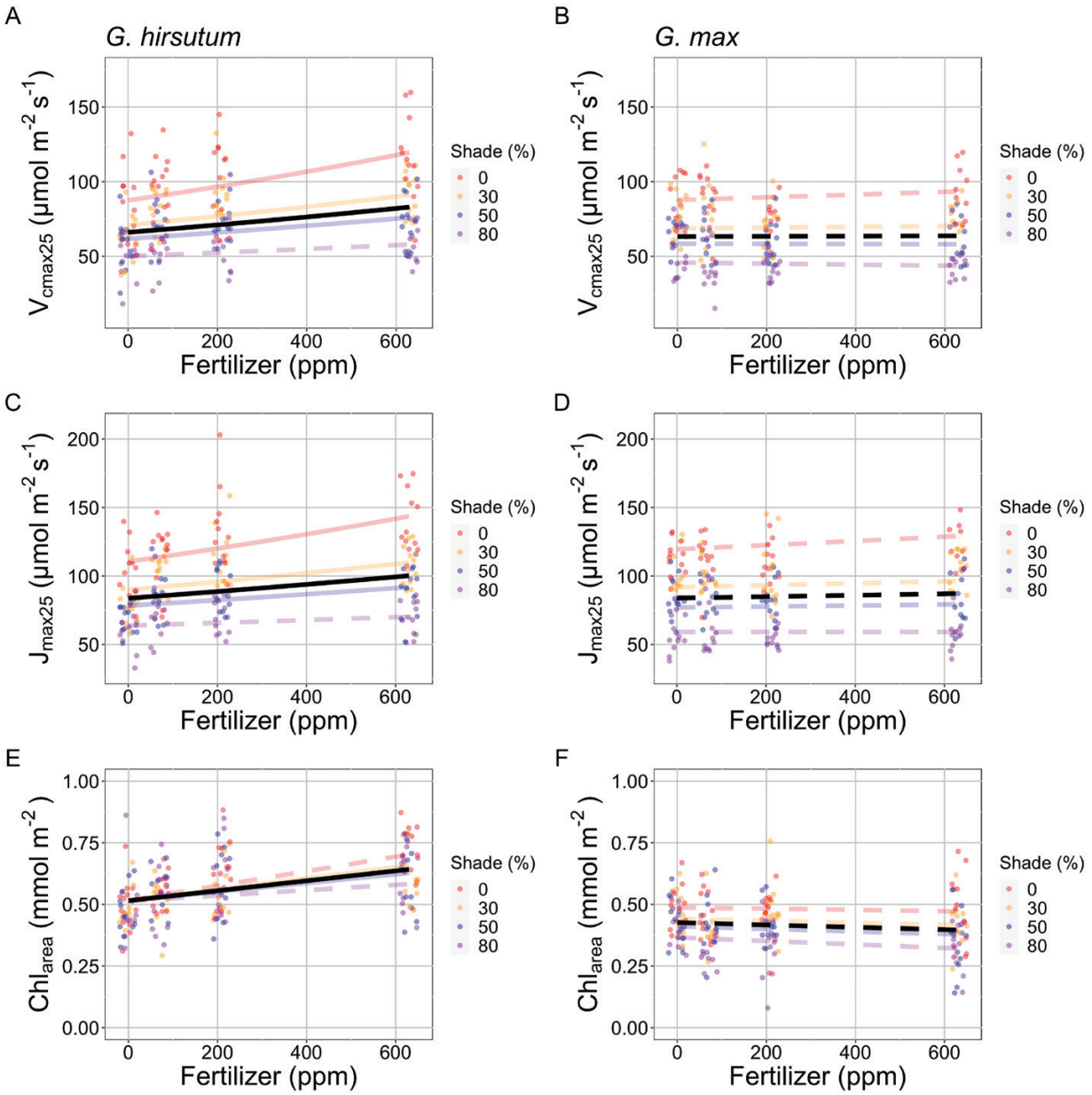

Fig. 2. The response of *G. hirsutum* (left panels) and *G. max* (right panels) V_{cmax25} (A, B), J_{max25} (C, D), and Chl_{area} (E, F) to nitrogen fertilization in the 0% (red), 30% (orange), 50% (blue), and 80% (purple) shade treatments. The dots represent individual data points and the lines are fitted lines from the linear mixed effects models at each shade treatment value. Separate lines are plotted for each shading treatment, with colors corresponding to the shading treatments. Solid lines are statistically significant trends ($P<0.05$) and dashed lines are non-significant trends ($P>0.05$). Because there was no fertilizer treatment by shading treatment interaction effect for any variable (Table 3), a black line is plotted to show the average trend across shading treatments for each species, and per shading treatments are shown as transparent lines. Nitrogen fertilizer amount (*x*-axis) is in parts per million (ppm) added twice per week and is jittered for visibility.

of soil nitrogen availability on photosynthetic processes in *G. max* (Fig. 2) contradicts these relationships and builds on previous work that calls the generality of these relationships into question (Ali *et al.*, 2015; Maire *et al.*, 2015; Dong *et al.*, 2017, 2020; Rogers *et al.*, 2017; Smith *et al.*, 2019; Paillassa *et al.*, 2020; Peng *et al.*, 2021).

Our results showed that the proportion of leaf nitrogen used for photosynthesis was reduced under increasing soil nitrogen availability (Fig. 3). This pattern was true for the fraction of leaf nitrogen allocated to Rubisco, bioenergetics, and light-harvesting components of photosynthesis, and did not differ between species. This result indicates that the relationship between leaf nitrogen and photosynthesis (Kattge *et al.*, 2009; Walker *et al.*, 2014) varies with soil nitrogen availability. Many land surface models that couple terrestrial carbon and nitrogen cycles simulate photosynthetic processes based on correlations with leaf

Table 4. ANOVA results for linear mixed effects model fit for dependent variables $\rho_{rubisco}$ (gN gN^{-1}), $\rho_{bioenergetics}$ (gN gN^{-1}), and $\rho_{lightharvesting}$ (gN gN^{-1})

		$\rho_{rubisco}$		$\rho_{bioenergetics}$		$\rho_{lightharvesting}$	
	df	χ^2	*P*-value	χ^2	*P*-value	χ^2	*P*-value
Species (Sp)	1	5.155	**0.023**	33.787	**<0.001**	46.26	**<0.001**
Shading (Sh)	1	19.355	**<0.001**	33.522	**<0.001**	1.909	0.167
Fertilizer (F)	1	9.491	**0.002**	13.375	**<0.001**	15.839	**<0.001**
Sp×Sh	1	0.188	0.664	0.244	0.621	0.354	0.552
Sp×F	1	0.042	0.838	0.833	0.362	0.017	0.897
Sh×F	1	0.145	0.704	0.708	0.400	0.01	0.92
Sp×Sh×F	1	0.067	0.795	0.143	0.706	0.227	0.634

df=degrees of freedom, χ^2=Wald's chi-squared statistic. *P*-values <0.05 are in bold.

nitrogen (e.g. Nemani *et al.*, 2009; Zaehle *et al.*, 2010, 2014; Lawrence *et al.*, 2019; Zhu *et al.*, 2019; reviewed in Smith and Dukes, 2013). Our results indicate that these relationships are not static with the environment and, if assumed to be static, may give erroneous predictions under changing soil nitrogen availability.

Additionally, the proportion of leaf nitrogen used for photosynthesis increased under increasing light availability (Fig. 3). This was true for the nitrogen in Rubisco and bioenergetic components of photosynthesis, but not the light-harvesting components. This confirms the results of previous studies (Pons and Pearcy, 1994; Evans and Poorter, 2001), although Evans and Poorter (2001) saw reduced relative allocation to light harvesting. This was an expected response based on classical qualitative theory (Boardman, 1977) and more recently quantified theory (Wang *et al.*, 2017; Smith *et al.*, 2019) of photosynthesis that suggests that plants acclimate to light availability by increasing investment in the enzymatic components of photosynthesis to maximize the use of available light for carbon assimilation. However, the present theory only predicts rates of enzymatically driven fluxes (e.g. V_{cmax25} and J_{max25}), but not the relative proportion of total leaf nitrogen invested in these processes. To improve carbon–nitrogen coupling in land surface models, the relative proportion must also be simulated (Ghimire *et al.*, 2017). Recent work combining theory and observational data provides a potential avenue for achieving this goal (Luo *et al.*, 2021).

Photosynthetic processes are more tightly coupled to light than to soil nitrogen availability

In support of our hypotheses, light availability tended to be a stronger driver of photosynthetic processes than soil nitrogen availability. While the treatments are not perfectly comparable, they do represent extreme high and low levels of each variable. On average across the two species, the light gradient ranging from a daily maximum of 489 μmol m^{-2} s^{-1} (80% shading) to 1662 μmol m^{-2} s^{-1} (0% shading) resulted in a 17% and 16% increase in V_{cmax25} and J_{max25}, respectively, while twice-per-week applications of 630 ppm N only increased V_{cmax25} and J_{max25} by 5% and 4%, respectively (Fig. 2). These results confirm that light availability is a strong driver of photosynthetic capacity (Boardman, 1977; Niinemets *et al.*, 2015; Poorter *et al.*, 2019).

A primary goal of our study was to use light availability as a proxy for photosynthetic demand and, in support of our first hypothesis, increases in light availability resulted in plants using more nitrogen to increase V_{cmax25} and J_{max25} (Fig. 2). Importantly, this happened consistently across all soil nitrogen availability treatments and in both species. This strongly indicates that plants adjust photosynthetic capacity to meet demands dictated by light availability irrespective of how much nitrogen is available to meet those demands, corroborating previous studies (Dong *et al.*, 2017, 2020; Poorter *et al.*, 2019). This comes at a clear distinction from the limited photosynthetic capacity response to soil nitrogen availability and, together, suggest that light (or other factors that influence photosynthetic demand) is more important for dictating per-leaf-area photosynthetic capacity than soil nitrogen availability. Many land surface models include light–photosynthesis relationships through the implementation of sun and shade portions of the canopy (Bonan *et al.*, 2021), but these results suggest that further consideration of spatial variability in sunlight across the land surface should also be considered for correctly modeling photosynthetic capacity.

One approach for predicting photosynthetic capacity responses to light availability is via eco-evolutionary optimality (Harrison *et al.*, 2021; Mengoli *et al.*, 2022). Photosynthetic theory based on these principles would suggest that V_{cmax25} and J_{max25} should scale proportionally with light availability (Dong *et al.*, 2017; Wang *et al.*, 2017; Smith *et al.*, 2019). However, that is not what we saw here. Instead, the light availability response, while strong, was more muted than expected (Fig. 2). Similarly muted responses have been observed along light availability gradients within plant canopies (Niinemets *et al.*, 2015). This may be the result of 'overinvestment' in photosynthetic capacity by shaded plants to allow them to quickly initiate photosynthesis when light becomes available (Meir *et al.*, 2002; Way and Pearcy, 2012; Buckley *et al.*, 2013), although this mechanism deserves further investigation. Nonetheless, this reflects a limitation to our understanding of plant photosynthetic investment that requires further investigation.

Whole-plant responses to soil nitrogen availability are greater than leaf-level responses

Supporting our hypotheses, both light and soil nitrogen availability increased the total leaf area and biomass in each species (Fig. 4). While this was not surprising given that light and nitrogen are well known to limit productivity (LeBauer and Treseder, 2008; Fay *et al.*, 2015; Harpole *et al.*, 2017; Menge

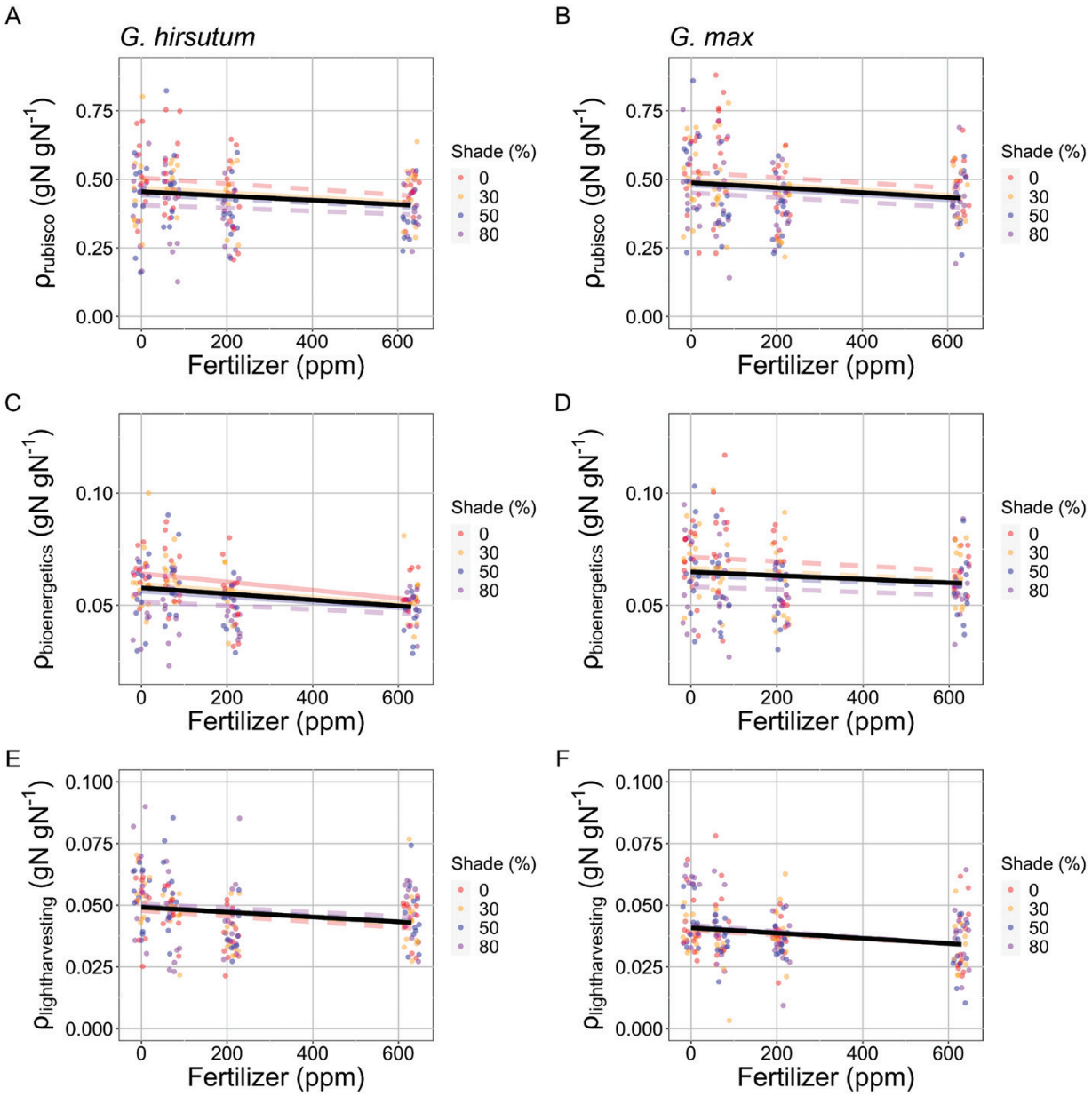

Fig. 3. The response of *G. hirsutum* (left panels) and *G. max* (right panels) $\rho_{rubisco}$ (A, B), $\rho_{bioenergetics}$ (C, D), and $\rho_{lightharvesting}$ (E, F) to nitrogen fertilization in the 0% (red), 30% (orange), 50% (blue), and 80% (purple) shade treatments. The dots represent individual data points and the lines are fitted lines from the linear mixed effects models at each shade treatment value. Solid lines are statistically significant trends ($P<0.05$) and dashed lines are non-significant trends ($P>0.05$). Separate lines are plotted for each shading treatment, with colors corresponding to the shading treatments. Because there was no fertilizer treatment by shading treatment interaction effect for any variable (Table 4), a black line is plotted to show the average trend across shading treatments for each species, and per shading treatments are shown as transparent lines. Nitrogen fertilizer amount (*x*-axis) is in parts per million (ppm) added twice per week and is jittered for visibility.

et al., 2017), the comparison of these responses with that of the leaf physiological responses can be used to better understand plant nitrogen and carbon allocation decisions.

Notably, and in support of our second hypothesis, the whole-plant responses to soil nitrogen availability (Fig. 4) were stronger and more consistent than the leaf-level responses (Figs 1–3). Similar results were found in a recent meta-analysis that compared effects of nitrogen addition on common leaf and whole-plant measurements (Liang *et al.*, 2020). This indicates that plants use added nitrogen preferentially to build new tissues, as opposed to increasing per-leaf-area photosynthetic enzymes. In our study, the primary tissues being built were for leaves, allowing the plant to access more light and therefore achieve greater whole-plant carbon assimilation. Similarly,

additional light also resulted in greater leaf area and biomass, reflecting the plants' allocation of increased carbon (due higher per-leaf-area photosynthesis) to enhanced light capture.

Table 5. ANOVA results for linear mixed effects model fit for dependent variables total leaf area (cm^2) and biomass (g)

		Total leaf area		Biomass	
	df	**χ^2**	***P*-value**	**χ^2**	***P*-value**
Species (Sp)	1	162.384	**<0.001**	1.905	0.168
Shading (Sh)	1	35.267	**<0.001**	230.163	**<0.001**
Fertilizer (F)	1	62.190	**<0.001**	51.259	**<0.001**
Sp×Sh	1	5.499	**0.019**	7.199	**0.007**
Sp×F	1	0.072	0.789	2.756	0.097
Sh×F	1	6.172	**0.013**	4.856	**0.028**
Sp×Sh×F	1	2.890	0.089	0.250	0.617

df=degrees of freedom, χ^2=Wald's chi-squared statistic. *P*-values <0.05 are in bold.

Our whole-plant responses can be more contextualized using the information about the individuals' structural carbon cost to acquire nitrogen, presented in Perkowski *et al.* (2021). Those results indicated that the individuals in our study, which were the same as those used in Perkowski *et al.* (2021), had lower structural carbon costs to acquire nitrogen when soil nitrogen fertilization increased, regardless of species. This response allowed individuals to increase whole-plant nitrogen uptake with lower below-ground carbon investments when there was more nitrogen available in the soil. These patterns probably resulted in an additional stimulation of biomass outside of what would be possible just from the added nutrients alone and also probably helped drive the increase in leaf area. These types of dynamic whole-plant allocation responses follow what is known from theory (Dybzinski *et al.*, 2011; Franklin *et al.*, 2012; Farrior *et al.*, 2013) and should be included in land surface models (e.g. as in Shi *et al.*, 2016; Zhu *et al.*, 2019; Braghiere *et al.*, 2022).

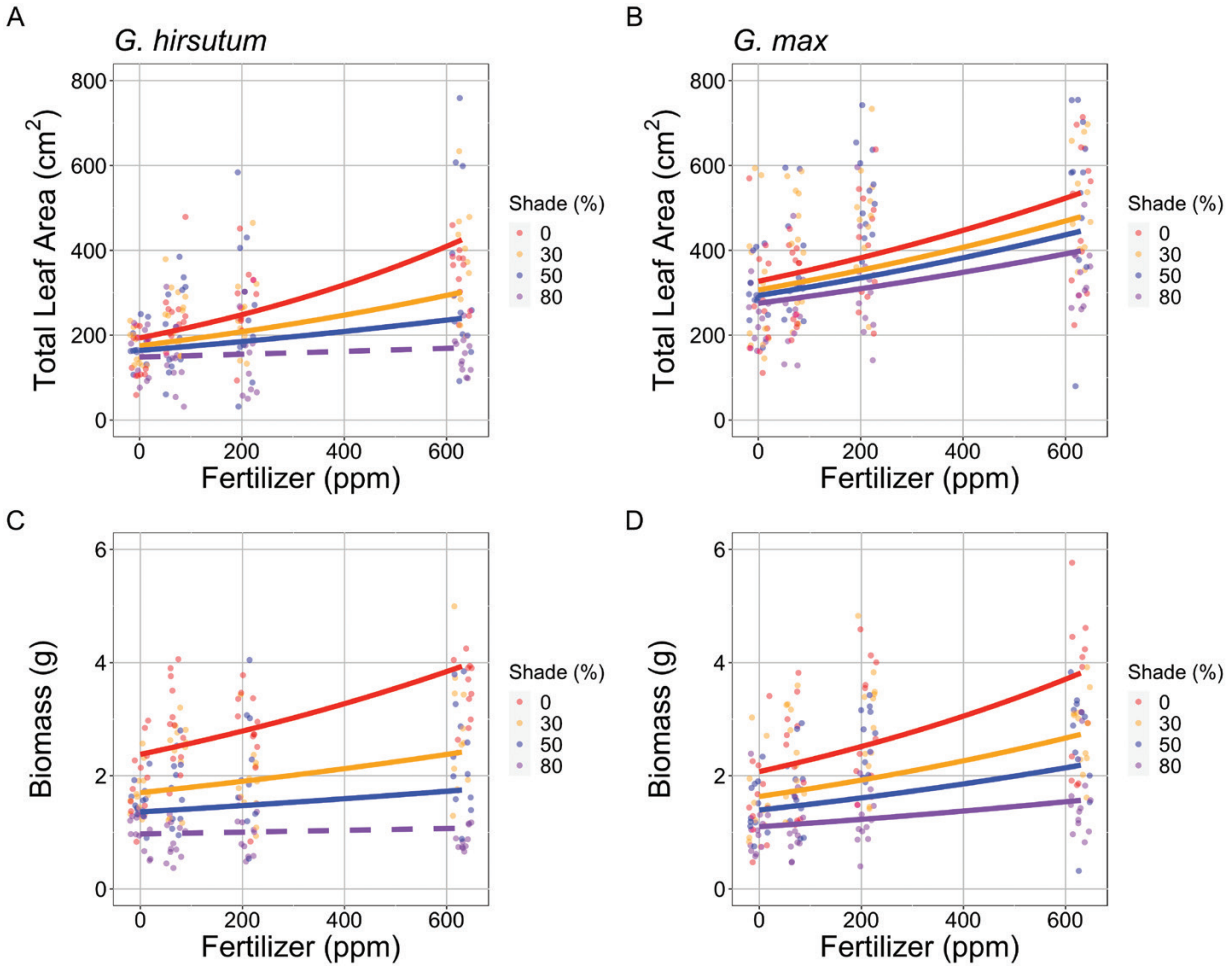

Fig. 4. The response of *G. histutum* (left panels) and *G. max* (right panels) total leaf area (A, B) and biomass (C, D) to nitrogen fertilization in the 0% (red), 30% (orange), 50% (blue), and 80% (purple) shade treatments. The dots represent individual data points and the lines are fitted lines from the linear mixed effects models at each shade treatment value. Solid lines are statistically significant trends ($P<0.05$) and dashed lines are non-significant trends ($P>0.05$). Separate lines are plotted for each shading treatment, with colors corresponding to the shading treatments. Nitrogen fertilizer amount (*x*-axis) is in parts per million (ppm) added twice per week and is jittered for visibility.

Study limitations

In the highest light (0% shading) and highest nitrogen (630 ppm) availability treatment combination, the biomass:pot volume ratio was greater than the 1 g l^{-1} recommended by Poorter *et al.* (2012) to avoid pot size limitation to growth and physiological processes. This was not the case for the other 15 treatment combinations. It is possible that pot size may have limited the responses seen in this treatment, which may have caused leaf and whole-plant responses to soil nitrogen fertilization and light availability to be underestimated. However, any potential pot size limitation in this treatment combination did not influence our qualitative results, which found that individuals grown under 0% shade and 630 ppm N had the greatest growth and fastest photosynthesis rates compared with any of the other treatment combinations. Future experiments should carefully select pot size to avoid additional factors that limit the interpretation of experimental results.

In our study, plants were well spaced in order to nullify potential light competition from neighboring plants. Therefore, our results may not hold for more closed canopy systems or in canopies of species with high leaf area indices. In these instances, increased light competition may reduce allocation to new growth under increased nitrogen availability if new growth would only result in self-shading. Thus, the increased nitrogen available may instead be preferentially allocated elsewhere (e.g. to photosynthetic processes). The results found here should be further validated in closed canopy systems or in species with complex canopy architectures.

The species differences found here and in Perkowski *et al.* (2021) suggest that nitrogen fertilization may have a more muted effect on growth and physiology in a plant that is capable of forming symbiotic associations with nitrogen-fixing bacteria (*G. max*) than a plant that is incapable of forming such associations (*G. hirsutum*). This may be due to changes in the strength of the association with differing levels of nitrogen availability, where increasing fertilization decreased plant investments in root nodulation and may have promoted nitrogen uptake through less costly direct uptake pathways (Perkowski *et al.*, 2021). However, we caution against assigning causality to these species differences due to the lack of phylogenetic relatedness and the different life history strategies of *G. max* (herbaceous annual) and *G. hirsutum* (woody perennial). If the nutrient acquisition strategy is the causal explanation for driving the interspecies variation observed in this experiment, future studies that examine these responses in a single species with and without the presence of symbiotic nitrogen-fixing bacteria would be a useful follow-up to address these patterns.

While species differed in the magnitude of their response to changing soil nitrogen availability and light availability, species did not differ with respect to the direction of their responses. Given additional life history trait differences between both species, similar directional responses could indicate that these patterns might be generalizable across species. In this study, we used crop seedlings with high growth rates, and thus high resource demands; however, it is possible that these results may not hold in less resource-demanding species. Thus, future work could consider using a greater number of species with different life history strategies to make generalizable claims about the impact of soil nitrogen availability and light availability on leaf nitrogen–photosynthesis relationships and how these relationships scale to whole-plant growth.

Conclusions

The results of our light by nitrogen availability experiment showed that, while nitrogen availability tended to increase leaf nitrogen, nitrogen availability consistently reduced the proportion of leaf nitrogen used for photosynthetic processes. This result suggests that the leaf nitrogen–photosynthesis relationship varies with soil nitrogen availability, contrasting with previous work and calling the use of these relationships in terrestrial biosphere models into question. Instead, plants tended to preferentially allocate increased nitrogen to the building of new tissues, specifically leaves. Light availability, on the other hand, consistently increased the proportion of leaf nitrogen used for photosynthetic processes. These results indicate that soil nitrogen availability strongly controls whole-plant processes, while leaf photosynthetic processes are more responsive to above-ground conditions. These responses should be included in coupled carbon–nitrogen models of terrestrial ecosystems.

Author contributions

EFW and NGS: design; EFW: carrying out the experiment; NGS: data analysis. All authors contributed to the interpretation of the results and writing of the manuscript.

Conflict of interest

None.

Funding

This work was supported by the National Science Foundation (DEB-2045968), Texas Tech University, and the LEMONTREE (Land Ecosystem Models based On New Theory, Observation and Experiments) project, which is funded through the generosity of Eric and Wendy Schmidt by recommendation of the Schmidt Futures programme.

Data availability

All data and R codes used for the analyses and figure creation can be found on Zenodo at: https://zenodo.org/record/7013894#.Y68bJOzMLlY (DOI: 10.5281/zenodo. 7469653; Perkowski *et al.*, 2022).

References

Ali AA, Xu C, Rogers A, *et al*. 2015. Global-scale environmental control of plant photosynthetic capacity. Ecological Applications **25**, 2349–2365.

Arneth A, Mercado L, Kattge J, Booth BBB. 2012. Future challenges of representing land-processes in studies on land–atmosphere interactions. Biogeosciences **9**, 3587–3599.

Barnes JD, Balaguer L, Manrique E, Elvira S, Davison AW. 1992. A reappraisal of the use of DMSO for the extraction and determination of chlorophylls a and b in lichens and higher plants. Environmental and Experimental Botany **32**, 85–100.

Bates D, Mächler M, Bolker B, Walker S. 2015. Fitting linear mixed-effects models using lme4. Journal of Statistical Software **67**, 1–48.

Bazzaz FA. 1990. The response of natural ecosystems to the rising global CO_2 levels. Annual Review of Ecology and Systematics **21**, 167–196.

Bernacchi CJ, Singsaas EL, Pimentel C, Portis Jr AR, Long SP. 2001. Improved temperature response functions for models of Rubisco-limited photosynthesis. Plant, Cell & Environment **24**, 253–259.

Berry J, Bjorkman O. 1980. Photosynthetic response and adaptation to temperature in higher plants. Annual Review of Plant Physiology **31**, 491–543.

Bialic-Murphy L, Smith NG, Voothuluru P, McElderry RM, Roche MD, Cassidy ST, Kivlin SN, Kalisz S. 2021. Invasion-induced root–fungal disruptions alter plant water and nitrogen economies. Ecology Letters **24**, 1145–1156.

Boardman NK. 1977. Comparative photosynthesis of sun and shade plants. Annual Review of Plant Physiology **28**, 355–377.

Bonan GB, Lawrence PJ, Oleson KW, Levis S, Jung M, Reichstein M, Lawrence DM, Swenson SC. 2011. Improving canopy processes in the Community Land Model version 4 (CLM4) using global flux fields empirically inferred from FLUXNET data. Journal of Geophysical Research **116**, G02014.

Bonan GB, Lombardozzi DL, Wieder WR, Oleson KW, Lawrence DM, Hoffman FM, Collier N. 2019. Model structure and climate data uncertainty in historical simulations of the terrestrial carbon cycle (1850–2014). Global Biogeochemical Cycles **33**, 1310–1326.

Bonan GB, Patton EG, Finnigan JJ, Baldocchi DD, Harman IN. 2021. Moving beyond the incorrect but useful paradigm: reevaluating big-leaf and multilayer plant canopies to model biosphere–atmosphere fluxes—a review. Agricultural and Forest Meteorology **306**, 108435.

Booth BBB, Jones CD, Collins M, Totterdell IJ, Cox PM, Sitch S, Huntingford C, Betts RA, Harris GR, Lloyd J. 2012. High sensitivity of future global warming to land carbon cycle processes. Environmental Research Letters **7**, 024002.

Braghiere RK, Fisher JB, Allen K, Brzostek E, Shi M, Yang X, Ricciuto DM, Fisher RA, Zhu Q, Phillips RP. 2022. Modeling global carbon costs of plant nitrogen and phosphorus acquisition. Journal of Advances in Modeling Earth Systems **14**, e2022-MS003204.

Buckley TN, Cescatti A, Farquhar GD. 2013. What does optimization theory actually predict about crown profiles of photosynthetic capacity when models incorporate greater realism? Plant, Cell & Environment **36**, 1547–1563.

Davies-Barnard T, Meyerholt J, Zaehle S, *et al*. 2020. Nitrogen cycling in CMIP6 land surface models: progress and limitations. Biogeosciences **17**, 5129–5148.

Dietze MC. 2014. Gaps in knowledge and data driving uncertainty in models of photosynthesis. Photosynthesis Research **119**, 3–14.

Dong N, Prentice IC, Evans BJ, Caddy-Retalic S, Lowe AJ, Wright IJ. 2017. Leaf nitrogen from first principles: field evidence for adaptive variation with climate. Biogeosciences **14**, 481–495.

Dong N, Prentice IC, Wright IJ, Evans BJ, Togashi HF, Caddy-Retalic S, McInerney FA, Sparrow B, Leitch E, Lowe AJ. 2020. Components of leaf-trait variation along environmental gradients. New Phytologist **228**, 82–94.

Dong N, Wright IJ, Chen JM, Luo X, Wang H, Keenan TF, Smith NG, Prentice IC. 2022. Rising CO_2 and warming reduce global canopy demand for nitrogen. New Phytologist **235**, 1692–1700.

Duursma RA. 2015. Plantecophys—an R package for analysing and modelling leaf gas exchange data. PLoS One **10**, e0143346.

Dybzinski R, Farrior C, Wolf A, Reich PB, Pacala SW. 2011. Evolutionarily stable strategy carbon allocation to foliage, wood, and fine roots in trees competing for light and nitrogen: an analytically tractable, individual-based model and quantitative comparisons to data. The American Naturalist **177**, 153–166.

Evans JR. 1989. Photosynthesis and nitrogen relationships in leaves of C_3 plants. Oecologia **78**, 9–19.

Evans JR, Clarke VC. 2019. The nitrogen cost of photosynthesis. Journal of Experimental Botany **70**, 7–15.

Evans JR, Poorter H. 2001. Photosynthetic acclimation of plants to growth irradiance: the relative importance of specific leaf area and nitrogen partitioning in maximizing carbon gain. Plant, Cell & Environment **24**, 755–767.

Evans JR, Seemann JR. 1989. The allocation of protein nitrogen in the photosynthetic apparatus: costs, consequences, and control. Photosynthesis **8**, 183–205.

Farquhar GD, von Caemmerer S, Berry JA. 1980. A biochemical model of photosynthetic CO2 assimilation in leaves of C_3 species. Planta **149**, 78–90.

Farrior CE, Tilman D, Dybzinski R, Reich PB, Levin SA, Pacala SW. 2013. Resource limitation in a competitive context determines complex plant responses to experimental resource additions. Ecology **94**, 2505–2517.

Fay PA, Prober SM, Harpole WS, *et al*. 2015. Grassland productivity limited by multiple nutrients. Nature Plants **1**, 15080.

Field CH, Mooney HA. 1986. Photosynthesis–nitrogen relationship in wild plants. In: Givnish TJ, ed. On the Economy of Plant Form and Function: Proceedings of the Sixth Maria Moors Cabot Symposium, Evolutionary Constraints on Primary Productivity, Adaptive Patterns of Energy Capture in Plants, Harvard Forest, August 1983. Cambridge: Cambridge University Press, 25–56.

Firn J, McGree JM, Harvey E, *et al*. 2019. Leaf nutrients, not specific leaf area, are consistent indicators of elevated nutrient inputs. Nature Ecology & Evolution **3**, 400–406.

Fox J, Weisberg S. 2019. An R companion to applied regression, 3rd edn. Thousand Oaks, CA: Sage.

Franklin O, Harrison SP, Dewar R, *et al*. 2020. Organizing principles for vegetation dynamics. Nature Plants **6**, 444–453.

Franklin O, Johansson J, Dewar RC, Dieckmann U, McMurtrie RE, Brännström A, Dybzinski R. 2012. Modeling carbon allocation in trees: a search for principles. Tree Physiology **32**, 648–666.

Friedlingstein P, Meinshausen M, Arora VK, Jones CD, Anav A, Liddicoat SK, Knutti R. 2014. Uncertainties in CMIP5 climate projections due to carbon cycle feedbacks. Journal of Climate **27**, 511–526.

Ghimire B, Riley WJ, Koven CD, Kattge J, Rogers A, Reich PB, Wright IJ. 2017. A global trait-based approach to estimate leaf nitrogen functional allocation from observations. Ecological Applications **27**, 1421–1434.

Harpole WS, Sullivan LL, Lind EM, *et al*. 2017. Out of the shadows: multiple nutrient limitations drive relationships among biomass, light and plant diversity. Functional Ecology **31**, 1839–1846.

Harrison SP, Cramer W, Franklin O, *et al*. 2021. Eco-evolutionary optimality as a means to improve vegetation and land-surface models. New Phytologist **231**, 2125–2141.

Hikosaka K. 2014. Optimal nitrogen distribution within a leaf canopy under direct and diffuse light. Plant, Cell & Environment **37**, 2077–2085.

Hoagland DR, Arnon DI. 1950. The water culture method for growing plants without soil. California Agricultural Experiment Station Circular 347. Berkley, CA.

Kattge J, Knorr W. 2007. Temperature acclimation in a biochemical model of photosynthesis: a reanalysis of data from 36 species. Plant, Cell & Environment **30**, 1176–1190.

Kattge J, Knorr W, Raddatz T, Wirth C. 2009. Quantifying photosynthetic capacity and its relationship to leaf nitrogen content for global-scale terrestrial biosphere models. Global Change Biology **15**, 976–991.

Keenan TF, Baker I, Barr A, *et al*. 2012. Terrestrial biosphere model performance for inter-annual variability of land–atmosphere CO_2 exchange. Global Change Biology **18**, 1971–1987.

Kenward MG, Roger JH. 1997. Small sample inference for fixed effects from restricted maximum likelihood. Biometrics **53**, 983–997.

Knorr W, Heimann M. 2001. Uncertainties in global terrestrial biosphere modeling: 1. A comprehensive sensitivity analysis with a new photosynthesis and energy balance scheme. Global Biogeochemical Cycles **15**, 207–225.

Langsrud O. 2003. ANOVA for unbalanced data: use Type II instead of Type III sums of squares. Statistics and Computing **13**, 163–167.

Lawrence DM, Fisher RA, Koven CD, *et al*. 2019. The Community Land Model Version 5: description of new features, benchmarking, and impact of forcing uncertainty. Journal of Advances in Modeling Earth Systems **11**, 4245–4287.

LeBauer DS, Treseder KK. 2008. Nitrogen limitation of net primary productivity in terrestrial ecosystems is globally distributed. Ecology **89**, 371–379.

Lenth RV. 2016. Least-squares means: the R package lsmeans. Journal of Statistical Software **69**, 1–33.

Li W, Zhang H, Huang G, Liu R, Wu H, Zhao C, McDowell NG. 2020. Effects of nitrogen enrichment on tree carbon allocation: a global synthesis. Global Ecology and Biogeography **29**, 573–589.

Liang X, Zhang T, Lu X, *et al*. 2020. Global response patterns of plant photosynthesis to nitrogen addition: a meta-analysis. Global Change Biology **26**, 3585–3600.

Luo X, Keenan TF. 2020. Global evidence for the acclimation of ecosystem photosynthesis to light. Nature Ecology and Evolution **4**, 1351–1357.

Luo X, Keenan TF, Chen JM, *et al*. 2021. Global variation in the fraction of leaf nitrogen allocated to photosynthesis. Nature Communications **12**, 4866.

Maire V, Wright IJ, Prentice IC, *et al*. 2015. Global effects of soil and climate on leaf photosynthetic traits and rates. Global Ecology and Biogeography **24**, 706–717.

Meir P, Kruijt B, Broadmeadow M, Barbosa E, Kull O, Carswell F, Nobre A, Jarvis PG. 2002. Acclimation of photosynthetic capacity to irradiance in tree canopies in relation to leaf nitrogen concentration and leaf mass per unit area. Plant, Cell & Environment **25**, 343–357.

Menge DNL, Batterman SA, Hedin LO, Liao W, Pacala SW, Taylor BN. 2017. Why are nitrogen-fixing trees rare at higher compared to lower latitudes? Ecology **98**, 3127–3140.

Mengoli G, Agustí-Panareda A, Boussetta S, Harrison SP, Trotta C, Prentice IC. 2022. Ecosystem photosynthesis in land-surface models: a first-principles approach incorporating acclimation. Journal of Advances in Modeling Earth Systems **14**, e2021MS002767.

Nemani R, Hashimoto H, Votava P, Melton F, Wang W, Michaelis A, Mutch L, Milesi C, Hiatt S, White M. 2009. Monitoring and forecasting ecosystem dynamics using the Terrestrial Observation and Prediction System (TOPS). Remote Sensing of Environment **113**, 1497–1509.

Niinemets U, Keenan TF, Hallik L. 2015. A worldwide analysis of within-canopy variations in leaf structural, chemical and physiological traits across plant functional types. New Phytologist **205**, 973–993.

Niinemets U, Kull O, Tenhunen JD. 1998. An analysis of light effects on foliar morphology, physiology, and light interception in temperate deciduous woody species of contrasting shade tolerance. Tree Physiology **18**, 681–696.

Niinemets U, Tenhunen JD. 1997. A model separating leaf structural and physiological effects on carbon gain along light gradients for the shade-tolerant species *Acer saccharum*. Plant, Cell & Environment **20**, 845–866.

Onoda Y, Wright IJ, Evans JR, Hikosaka K, Kitajima K, Niinemets U, Poorter H, Tosens T, Westoby M. 2017. Physiological and structural tradeoffs underlying the leaf economics spectrum. New Phytologist **214**, 1447–1463.

Paillassa J, Wright IJ, Prentice IC, *et al*. 2020. When and where soil is important to modify the carbon and water economy of leaves. New Phytologist **228**, 121–135.

Peng Y, Bloomfield KJ, Cernusak LA, Domingues TF, Prentice IC. 2021. Global climate and nutrient controls of photosynthetic capacity. Communications Biology **4**, 462.

Perkowski EA, Waring EF, Smith NG. 2021. Root mass carbon costs to acquire nitrogen are determined by nitrogen and light availability in two species with different nitrogen acquisition strategies. Journal of Experimental Botany **72**, 5766–5776.

Perkowski EA, Waring EF, Smith NG. 2022. Data from: Light-by-nitrogen greenhouse experiment dataset and R code (v2.0). Zenodo https://doi.org/10.5281/zenodo.7013894

Pons TL, Pearcy RW. 1994. Nitrogen reallocation and photosynthetic acclimation in response to partial shading in soybean plants. Physiologia Plantarum **92**, 636–644.

Poorter H, Bühler J, Van Dusschoten D, Climent J, Postma JA. 2012. Pot size matters: a meta-analysis of the effects of rooting volume on plant growth. Functional Plant Biology **39**, 839–850.

Poorter H, Knopf O, Wright IJ, Temme AA, Hogewoning SW, Graf A, Cernusak LA, Pons TL. 2022. A meta-analysis of responses of C_3 plants to atmospheric CO_2: dose–response curves for 85 traits ranging from the molecular to the whole-plant level. New Phytologist **233**, 1560–1596.

Poorter H, Niinemets U, Ntagkas N, Siebenkäs A, Mäenpää M, Matsubara S, Pons T. 2019. A meta-analysis of plant responses to light intensity for 70 traits ranging from molecules to whole plant performance. New Phytologist **223**, 1073–1105.

Prentice IC, Dong N, Gleason SM, Maire V, Wright IJ. 2014. Balancing the costs of carbon gain and water transport: testing a new theoretical framework for plant functional ecology. Ecology Letters **17**, 82–91.

R Core Team. 2019. R: a language and environment for statistical computing. Vienna, Austria: R Foundation for Statistical Computing.

Rogers A. 2014. The use and misuse of $V_{c,max}$ in Earth System Models. Photosynthesis Research **119**, 15–29.

Rogers A, Medlyn BE, Dukes JS, *et al*. 2017. A roadmap for improving the representation of photosynthesis in Earth system models. New Phytologist **213**, 22–42.

Sage RF, Kubien DS. 2007. The temperature response of C_3 and C_4 photosynthesis. Plant, Cell & Environment **30**, 1086–1106.

Schneider CA, Rasband WS, Eliceiri KW. 2012. NIH Image to ImageJ: 25 years of image analysis. Nature Methods **9**, 671–675.

Shi M, Fisher JB, Brzostek ER, Phillips RP. 2016. Carbon cost of plant nitrogen acquisition: global carbon cycle impact from an improved plant nitrogen cycle in the Community Land Model. Global Change Biology **22**, 1299–1314.

Smith NG, Dukes JS. 2013. Plant respiration and photosynthesis in global-scale models: incorporating acclimation to temperature and CO_2. Global Change Biology **19**, 45–63.

Smith NG, Keenan TF, Prentice IC, *et al*. 2019. Global photosynthetic capacity is optimized to the environment. Ecology Letters **22**, 506–517.

Smith NG, Lombardozzi D, Tawfik A, Bonan G, Dukes JS. 2017. Biophysical consequences of photosynthetic temperature acclimation for climate. Journal of Advances in Modeling Earth Systems **9**, 536–547.

Smith NG, Malyshev SL, Shevliakova E, Kattge J, Dukes JS. 2016. Foliar temperature acclimation reduces simulated carbon sensitivity to climate. Nature Climate Change **6**, 407–411.

Terrer C, Vicca S, Stocker BD, Hungate BA, Phillips RP, Reich PB, Finzi AC, Prentice IC. 2018. Ecosystem responses to elevated CO_2 governed by plant–soil interactions and the cost of nitrogen acquisition. New Phytologist **217**, 507–522.

Walker AP, Beckerman AP, Gu L, Kattge J, Cernusak LA, Domingues TF, Scales JC, Wohlfahrt G, Wullschleger SD, Woodward FI. 2014. The relationship of leaf photosynthetic traits—Vcmax and Jmax—to leaf nitrogen, leaf phosphorus, and specific leaf area: a meta-analysis and modeling study. Ecology and Evolution **4**, 3218–3235.

Wang H, Prentice IC, Keenan TF, Davis TW, Wright IJ, Cornwell WK, Evans BJ, Peng C. 2017. Towards a universal model for carbon dioxide uptake by plants. Nature Plants **3**, 734–741.

Way DA, Pearcy RW. 2012. Sunflecks in trees and forests: from photosynthetic physiology to global change biology. Tree Physiology **32**, 1066–1081.

Wellburn AR. 1994. The spectral determination of chlorophylls a and b, as well as total carotenoids, using various solvents with spectrophotometers of different resolution. Journal of Plant Physiology **144**, 307–313.

Westerband AC, Wright IJ, Maire V, *et al*. 2023. Coordination of photosynthetic traits across soil and climate gradients. Global Change Biology **29**, 856–873.

Wright IJ, Reich PB, Cornelissen JHC, *et al*. 2005. Assessing the generality of global leaf trait relationships. New Phytologist **166**, 485–496.

Wright IJ, Reich PB, Westoby M. 2003. Least-cost input mixtures of water and nitrogen for photosynthesis. The American Naturalist **161**, 98–111.

Yamori W, Hikosaka K, Way DA. 2014. Temperature response of photosynthesis in C_3, C_4, and CAM plants: temperature acclimation and temperature adaptation. Photosynthesis Research **119**, 101–117.

Zaehle S, Friedlingstein P, Friend AD. 2010. Terrestrial nitrogen feedbacks may accelerate future climate change. Geophysical Research Letters **37**, L01401.

Zaehle S, Medlyn BE, De Kauwe MG, *et al*. 2014. Evaluation of 11 terrestrial carbon-nitrogen cycle models against observations from two temperate Free-Air CO_2 Enrichment studies. New Phytologist **202**, 803–822.

Zhu Q, Riley WJ, Tang J, Collier N, Hoffman FM, Yang X, Bisht G. 2019. Representing nitrogen, phosphorus, and carbon interactions in the E3SM land model: development and global benchmarking. Journal of Advances in Modeling Earth Systems **11**, 2238–2258.

Ziehn T, Kattge J, Knorr W, Scholze M. 2011. Improving the predictability of global CO_2 assimilation rates under climate change. Geophysical Research Letters **38**.